Taylor & Francis
Taylor & Francis Group

Journal of Nuclear Science and Technology

ISSN: (Print) (Online) Journal homepage: https://www.tandfonline.com/loi/tnst20

Neutron capture cross-section measurement by mass spectrometry for Pb-204 irradiated in JRR-3

Shoji Nakamura, Yuji Shibahara, Atsushi Kimura, Shunsuke Endo & Toshiyuki Shizuma

To cite this article: Shoji Nakamura, Yuji Shibahara, Atsushi Kimura, Shunsuke Endo & Toshiyuki Shizuma (2023) Neutron capture cross-section measurement by mass spectrometry for Pb-204 irradiated in JRR-3, Journal of Nuclear Science and Technology, 60:9, 1133-1142, DOI: 10.1080/00223131.2023.2172088

To link to this article: https://doi.org/10.1080/00223131.2023.2172088

Published online: 13 Feb 2023.

JOURNAL OF NUCLEAR SCIENCE AND TECHNOLOGY
2023, VOL. 60, NO. 9, 1133–1142
https://doi.org/10.1080/00223131.2023.2172088

ARTICLE

Neutron capture cross-section measurement by mass spectrometry for Pb-204 irradiated in JRR-3

Shoji Nakamura[a], Yuji Shibahara[b], Atsushi Kimura[a], Shunsuke Endo[a] and Toshiyuki Shizuma[c]

[a]Nuclear Science and Engineering Center, Japan Atomic Energy Agency, Tokai-mura, Naka-gun, Japan; [b]Division of Nuclear Engineering Science, Institute for Integrated Radiation and Nuclear Science, Kyoto University, Sennan-gun, Osaka, Japan; [c]Tokai Quantum Beam Science Center, National Institutes for Quantum Science and Technology, Tokai-mura Naka-gun, Japan

ABSTRACT

Reliable neutron capture cross sections of lead isotopes are necessary for the development of lead or lead-bismuth cooled fast reactors. Although ^{204}Pb has the smallest natural abundance in stable Pb isotopes, its neutron capture cross-section data are important because a long-lived radionuclide ^{205}Pb ($T_{1/2} = 17.3$ million years) is produced by a neutron capture reaction on ^{204}Pb. This study applied a mass spectrometry method to measure the neutron capture cross section of ^{204}Pb. An enriched ^{204}Pb sample was irradiated for 24 days with a neutron flux on the order of 10^{13} $n/cm^2/sec$ at the Japan Research Reactor-3. The irradiated ^{204}Pb sample was analyzed by thermal ionization mass spectrometry to obtain the isotopic ratio between ^{205}Pb and ^{204}Pb. Consequently, the thermal-neutron capture cross-section of ^{204}Pb was found to be 0.536 ± 0.030 barns.

ARTICLE HISTORY
Received 21 September 2022
Accepted 12 January 2023

KEYWORDS
Lead-204; lead-205; mass spectrometry; activation method; JRR-3

1. Introduction

An innovative nuclear power system that can serve as a core energy resource has been studied by integrating economic performance, safety, sustainability, and nuclear non-proliferation resistance. The Generation-IV International Forum [1,2] was established as a framework for international cooperation on research and development. The GEN-IV has considered lead-cooled fast reactors (LFRs) as one of the reactor types for innovative nuclear systems due to the following advantages: (a) it is not necessary to make a reactor vessel to withstand high pressure because Pb has a high boiling point of 1,749°C; (b) the neutron economy is good due to the small neutron deceleration effect of Pb; (c) cooling capacity is high due to its high thermal conductivity; (d) due to its low reactivity with oxygen and water, Pb cooling is much safer than Na cooling in the case of leakage.

Accurate nuclear data are required for the design of LFRs; a reduction of the 20% uncertainty to 10% is required in the neutron energy region from 2 keV to 9 keV in energy-dependent neutron capture cross-sections of Pb [3]. In order to derive the absolute values of the energy-dependent neutron capture cross-sections, normalization has to be carried out. As one method, if there is one point of highly accurate cross-section data in the thermal-neutron energy region, it could be used for normalization. Based on this logic, we examined the measurement of the thermal-neutron capture cross-section for Pb. Lead-206 and lead-207 are candidates in terms of their abundances, but lead-204 was taken up in this study. This is because although the natural abundance of ^{204}Pb is small (1.4%), neutron cross-section data are of importance because a long-lived radionuclide ^{205}Pb ($(1.73 \pm 0.07) \times 10^7$ years [4]) is produced through a neutron capture reaction on ^{204}Pb and the accumulation of ^{205}Pb may cause long-lasting radiotoxicity. However, it is difficult to measure the neutron capture cross section by a conventional activation method because the radioactivity of the reaction product ^{205}Pb is too weak to be observed. To measure the neutron capture cross section of ^{204}Pb, we therefore applied mass spectrometry which enables us to estimate the amount of the reaction product ^{205}Pb in an irradiated Pb sample.

In the present work, an enriched ^{204}Pb sample was irradiated for a long period with thermal neutrons available in the Japan Research Reactor-3 (JRR-3) [5]. After irradiation, the sample was analyzed by thermal ionization mass spectrometry (TIMS) technique [6–8] at the Integral Radiation and Nuclear Science, Kyoto University (KURNS) [9]. The thermal-neutron capture cross section of ^{204}Pb was determined from the isotopic ratio between ^{205}Pb and ^{204}Pb and measured neutron flux. The present neutron capture cross section of ^{204}Pb was compared with earlier cross section data as well as evaluated values.

CONTACT Shoji Nakamura nakamura.shoji@jaea.go.jp Nuclear Data Center, Nuclear Science and Reactor Engineering Division, Nuclear Science and Engineering Center, Japan Atomic Energy Agency, 2-4 Shirakata, Ibaraki-ken, Tokai-mura, Naka-gun 319-1195, Japan

2. Experiment

2.1. Target preparation

A metallic ^{204}Pb sample enriched to 99.94%, purchased from ISOFLEX USA (San Francisco, CA, United States), was cut into two small pieces of 15.13 mg (sample A) and 13.18 mg (sample B) in weight. Only sample A was irradiated with neutrons. Mass analysis of both the irradiated and non-irradiated samples was carried out to obtain the amount of ^{205}Pb produced by neutron capture on ^{204}Pb. More details will be described in *Subsection 3.2*.

As shown in Figure 1, the sample A was rapped with a high-purity Al foil with a thickness of 15 μm to serve as a 'Pb target.' The Pb target was further wrapped with the Al foil in a twisted manner for fixing the position of the Pb target in a capsule made of aluminum and for removing heat due to gamma-rays in the reactor. The capsule has a diameter of 32 mm and a length of 150 mm. A set of two gold-aluminum (Au-Al) alloy wires with weights of 0.5 mg and 1.0 mg and a 1.2 mg molybdenum (Mo) metal foil was used to monitor a neutron flux ('monitor target'). We prepared two capsules containing a set of these monitors. While the Au-Al alloy wires serve as a monitor of the thermal-neutron flux component, the Mo foil serves as a monitor of the epi-thermal neutron flux component. Similar to the Pb target, the monitor target was further wrapped with the Al foil to form a twist before setting into an irradiation capsule. Two sets of the monitor capsules were irradiated before and after irradiation of the Pb target to confirm the stability of the neutron flux. Information on flux monitors is summarized in Table 1. Each irradiation capsule contained a hollow cylindrical Al spacer and a cylindrical Al weight so that it does not float in an irradiation hole. Since it was verified by numerical calculations using the ORIGEN2 code *version 2.2* [10] that the temperature of the capsule was kept at approximately 52°C in the cooling water with the temperature of 50°C, the Pb sample did not melt during neutron irradiation.

2.2. Neutron irradiation in JRR-3

Since the neutron capture cross-section of ^{204}Pb is small, long-term neutron irradiation with a large flux is required to produce an enough amount of ^{205}Pb for mass spectrometry. Such neutron irradiation is possible in the JRR-3 facility. Since the first criticality in 1962, the JRR-3 operated at a 20-MW thermal power has been utilized for nuclear engineering research and development such as neutron beam experiments, irradiation tests for nuclear fuels and materials, and also production of radio isotopes and silicon semiconductors [5]. The JRR-3 had been suspended since 2011 due to compliance with new regulatory standards for nuclear power plants but has resumed operation since the end of June 2021. Figure 2 shows the layout of irradiation facilities of the JRR-3. A hydraulic irradiation facility (HR) located in a heavy water reflector permits neutron irradiation in the range of 10 minutes to one cycle (26 days). In our preliminary experiments, it was found that the cadmium ratio was 5 from the reaction rates obtained by irradiating the Au/Al alloy wires with and without a 1-mm-thick Cd shield. The proportion of epi-thermal neutron flux component to total neutron flux was less than 1%. Hence, the HR can be considered as a well-thermalized neutron field. The HR equipment has HR-1 and HR-2 irradiation holes. HR-2 was selected in this experiment because it can be

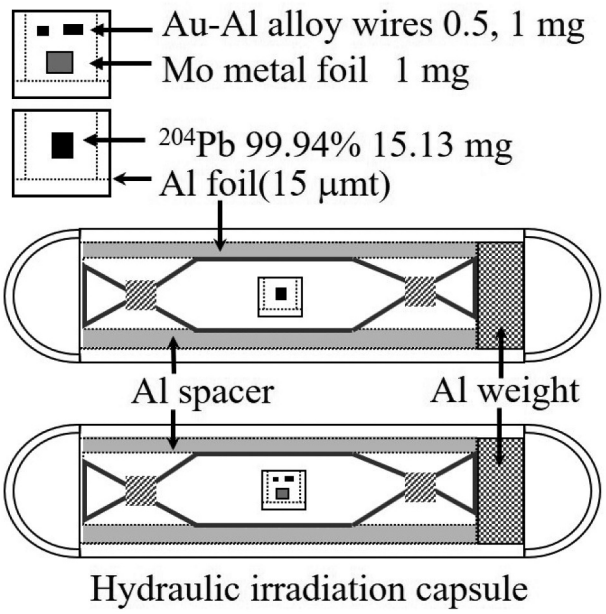

Figure 1. Schematic of capsules which contain irradiation targets of Pb and monitor samples.

Table 1. Information on neutron flux monitors.

Targets	Materials	Shape and size*	Weight (mg)	Abundance (%)	Purity (%)
Monitor Set #1	Au-Al alloy wires	0.510 mm Φ	0.572 ± 0.01	0.112 ± 0.001†	99.9845
			1.101 ± 0.01		
	^{98}Mo Metal foil	3 × 3 mm, 25 μm^{t}	1.191 ± 0.01	24.4 ± 0.1	99.95
Monitor Set #2	Au-Al alloy wires	0.510 mm Φ	0.581 ± 0.01	0.112 ± 0.001†	99.9845
			0.927 ± 0.01		
	^{98}Mo Metal foil	3 × 3 mm, 25 μm^{t}	1.204 ± 0.01	24.4 ± 0.1	99.95

Note: * The symbol 'Φ' represents the diameter and 't' the thickness. †Abundance of ^{197}Au.

used exclusively for a one-cycle period. When the JRR-3 started in 20-MW operation, the monitor target was transferred into the HR-2 and then irradiated for 30 minutes. Subsequently, the capsule containing the Pb target was transferred and irradiated for 576 hours (24 days). After the irradiation of the Pb target, another monitor target was irradiated for 30 minutes.

2.4. Gamma-ray measurement

After a cooling time of 95 hours, the irradiated capsules were sequentially transferred to a refill cell for opening them. The monitor and Pb target samples were collected, and then they were kept inside different polyethylene bags one at a time within a ventilation hood and heat-sealed. The surface of the Pb sample was oxidized and blackened, but the state of the foil was maintained. Gamma-ray measurement of the monitors was performed using a high-purity Ge detector (model GX2018–7500SL; MIRION Technologies (Canberra), Inc., United States) installed in the first experimental facility of the JRR-3. Its detector performance was characterized by a relative efficiency of 20% to that of a 7.6 cm × 7.6 cm Φ NaI(Tl) detector and an energy resolution of 1.8 keV full width at half maximum at the 1.33-MeV gamma-ray peak of ^{60}Co. The detector head was housed in a 5-cm-thick Pb shield box lined with 5-mm-thick copper plates. An acrylic sample stage was set at a distance of 100 mm from the front of the detector head. Photopeak efficiencies at this distance were obtained with the ^{152}Eu calibration source (EU402) with a 1.3% uncertainty and also ^{137}Cs and ^{60}Co in the mixed source (MX402) with a 1.3% uncertainty, which were supplied by the Japan Radioisotope Association. The depth of the active area in the calibration source was 1.5 mm. When measuring the samples, a 1.5-mm-thick acrylic plate was put on the sample stage to correct the measurement distance.

3. Analysis

3.1. Neutron flux

Neutron flux components were derived from the reaction rates R of the monitors obtained from γ-ray spectral data using the following equation [11]:

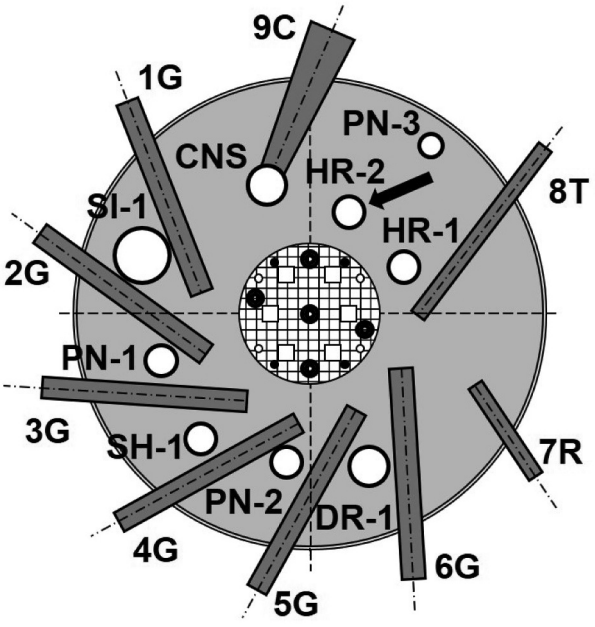

Figure 2. Various irradiation facilities around the reactor core of the JRR-3. The No. 2 hydraulic irradiation hole (HR-2) indicated by the arrow was used in the present irradiation.

Table 2. Results of the reaction rates of the monitors together with the measurement data [12].

Monitor set		Irradiation time T_{irr} (sec)	Cooling time T_c (sec)	Live time T_L (sec)	Real time T_R (sec)	Photo-peak Y_p (counts)	Half-life* (days)	γ-ray energy E_γ (keV)	Emission probability $I\gamma$ (%)	γ-ray self-shielding G_γ	Photo-peak efficiency ε_γ (%)	Reaction rate† R (1/sec)
#1	^{197}Au	1,800	524,135	900	902	44,806 ± 212	2.6943 ± 0.0003	411.8	95.62 ± 0.06	0.997	0.280 ± 0.004	(8.502 ± 0.142) ×10^{-9}
			531,380	2,760	2,770	256,186 ± 508						(8.440 ± 0.137) ×10^{-9}
											Weighted average	(8.449 ± 0.137) ×10^{-9}
	^{98}Mo	1,800	525,635	4,392	4,407	24,865 ± 158	2.7479 ± 0.0006	739.5	12.13 ± 0.22	0.998	0.161 ± 0.002	(1.433 ± 0.030) ×10^{-11}
#2	^{197}Au	1,805	340,724	601	603	54,753 ± 234	2.6943 ± 0.0003	411.8	95.62 ± 0.06	0.997	0.287 ± 0.004	(8.619 ± 0.143) ×10^{-9}
			341,684	601	604	88,424 ± 298						(8.743 ± 0.143) ×10^{-9}
											Weighted average	(8.695 ± 0.142) ×10^{-9}
	^{98}Mo	1,805	342,695	10,000	10,063	105,357 ± 326	2.7479 ± 0.0006	739.5	12.13 ± 0.22	0.998	0.166 ± 0.002	(1.511 ± 0.031) ×10^{-11}

Note: * Decay constants were calculated from half-lives. †Including systematic uncertainties.

$$R = \frac{\lambda_1 Y_1 \left(1/G_\gamma\right)}{n_0 I_{\gamma 1} \varepsilon_{\gamma 1} (1 - \exp(-\lambda_1 t_{irr})) \cdot \exp(-\lambda_1 t_c) \cdot (1 - \exp(-\lambda_1 t_R))} \cdot \frac{t_R}{t_L} \quad (1)$$

where subscripts *0* and *1* denote the target nuclide and reaction product, respectively. The symbol n is the number of parent nuclei in the monitor; I_γ is the γ-ray emission probability; ε_γ is its photo-peak efficiency; λ is the decay constant. The symbol t_{irr} represents the irradiation time, t_c the interval time from the end of irradiation to the start of measurement, t_R (t_L) is the real (live) time of γ-ray measurement; Y is the photo-peak counts after Compton subtraction; G_γ is the γ-ray self-shielding coefficient. Table 2 summarizes the results of reaction rates and information on γ-ray measurements for the monitors [12].

Based on *Westcott's* convention [13,14], the reaction rate R can be expressed by the following form [11]:

$$R = \sigma_0 \left(g G_{th} \phi_1 + G_{epi} \phi_2 s_0\right) \quad (2)$$

where the symbol σ_0 is the thermal-neutron capture cross section; g is the factor as a function of the temperature related to the departure of the cross-section behavior from the 1/υ law. The symbols G_{th} and G_{epi} denote self-shielding coefficients for thermal- and epi-thermal neutrons, respectively. The symbol Φ_1 (Φ_2) is a neutron flux component in the thermal (epi-thermal) energy region. The parameter s_0 represents the sensitivity of a nuclide to epi-thermal neutrons. Table 3 lists the results of neutron flux components $R/(gG_{\rm th}\sigma_0)$ together with nuclear data [15] used in analysis. Figure 3 shows the obtained neutron flux components plotted against the parameters s_0. The measurement data in Figure 3 were fitted with a linear function. The y-intercept at zero sensitivity to epi-thermal neutrons gives the thermal-neutron flux component. Table 4 summarizes the obtained y-intercepts and slopes. The thermal-neutron fluxes were obtained as $(7.55 \pm 0.26) \times 10^{13}$ n/cm^2/sec at the first day of the one-cycle operation and $(7.57 \pm 0.27) \times 10^{13}$ n/cm^2/sec at the last day of the operation. More details on the derivation of the thermal neutron flux are described in Ref [11]. The amount obtained by dividing the slope by the thermal-neutron flux component gives *Westcott*'s index [13,14], that is, the ratio of epi-thermal neutron flux component to the neutron flux. The index was at most 0.7 ~ 0.9% which is consistent with the interpretation that the neutron field in HR-2 is well thermalized.

Figure 4 shows the hourly data of thermal power during the irradiation, which provide an average power of 19.1 MW. The thermal powers during irradiation of the monitor sets #1 and #2 were 18.8 and 19.1 MW, respectively. The ratio between these powers is 0.95, and the ratio between the reaction rates in Table 2 is 0.97 ± 0.02; these ratios are in agreement within the uncertainty. The neutron flux can therefore be considered to be proportional to the thermal power. Consequently, the average neutron flux of $(7.57 \pm 0.27) \times 10^{13}$ n/cm^2/sec was obtained to yield the net amount of neutrons during irradiation of ^{204}Pb.

3.2. Mass analysis for Pb samples

The unirradiated and irradiated Pb samples were transferred to KURNS for mass analysis. The isotopic ratios of Pb sample were analyzed by TIMS. The mass analysis was performed using the mass spectrometer TRITON-T1 [6–8,16] (Thermo Fisher Scientific, Inc. USA) installed at KURNS [9]. Isotope analysis using TIMS was performed with silica gel and phosphoric acid as additives by the single filament method of a rhenium filament [17–19]. Since the Pb sample was a neutron activated sample, its amount had to be much less than the sample amount normally used for the mass analysis so as not to contaminate the mass spectrometer. There was also a problem of silica gel used as an additive; the silica gel was different from the one used widely for Pb isotopic ratio analysis [20,21]. This is why the beam intensity of Pb was much weaker than that used in the usual analysis. High-precision analysis of Pb isotopic ratio including evaluation of isotopic fractionation effect often utilizes the isotope dilution method ('double spike method' [19]) that spikes two types of isotopes. In a sense, this measurement would analyze the Pb isotope sample itself used for spikes. This is why the isotope dilution method was not used in this analysis. Instead, isotopic ratio analysis was carried out by normalization [17–19] using the linear mass discrimination law. The TIMS was operated according to the manner reported in Refs [19–21]: manners of loading a sample into the filament,

Table 3. Results of the neutron flux components together with nuclear data [15] used in the analysis.

Nuclide	σ_0 (barn)	s_0	g	Self-shielding G_{th}	Self-shielding G_{epi}	Flux component† $R/(gG_{th}\sigma_0)$ (n/cm^2/sec) Monitor Set #1	Monitor Set #2
^{197}Au	98.65 ± 0.09	17.22	1.0054	1.000	1.000	(8.573 ± 0.144) ×10^{13}	(8.690 ± 0.145) ×10^{13}
						(8.509 ± 0.138) ×10^{13}	(8.815 ± 0.145) ×10^{13}
					Weighted average	(8.519 ± 0.138) ×10^{13}	(8.766 ± 0.143) ×10^{13}
^{98}Mo	0.134 ± 0.003* (0.130 ± 0.006)	55.91	1.001	0.998	1.000	(1.070 ± 0.033) ×10^{14}	(1.145 ± 0.035) ×10^{14}

Note: * Previous our data for Mo. † Including systematic uncertainties.

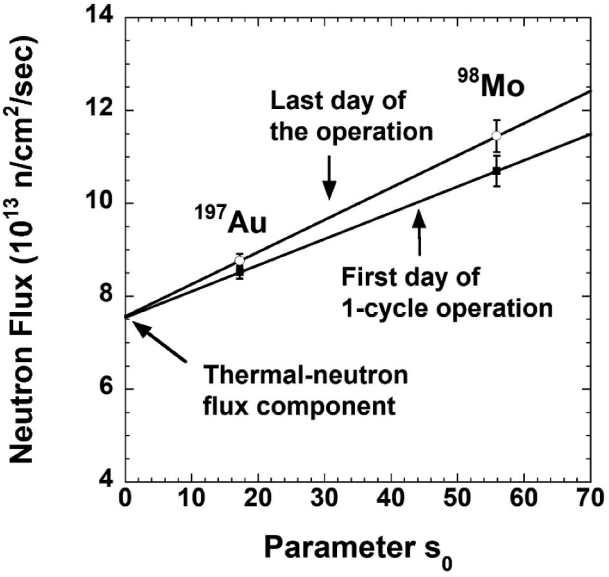

Figure 3. Neutron flux components at HR-2 obtained by the flux monitors.

Table 4. Results of the y-intercepts and slopes giving neutron flux components.

Irradiation	y-intercept (10^{13} n/cm^2/sec)	Slope (10^{13} n/cm^2/sec)	*Westcott*'s index [13] (%)
First day of one-cycle operation	7.547 ± 0.258	0.0564 ± 0.0101	0.7 ± 0.1
Last day of one-cycle operation	7.572 ± 0.274	0.0694 ± 0.0109	0.9 ± 0.1

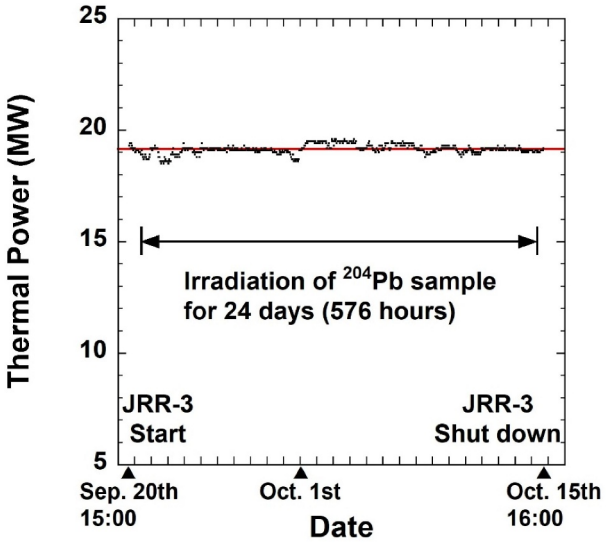

Figure 4. Fluctuations in the reactor thermal power of JRR-3 during one-cycle operation. The thermal-power data are plotted every hour over a period of one cycle operation.

optimizing ion current and the ion lens system, heading process of the filament, and so on. The effectiveness of the present method was first examined with the standard reference material of Pb (SRM981). Table 5 summarizes the analysis results obtained by normalization based on the ^{208}Pb/^{206}Pb ratio (=2.1681 [18,22]) together with the certified values. The present results were in good agreement with the certified values within the margin of uncertainty.

In the analysis of the unirradiated Pb sample, the ratio of the yields between the mass 205 and 203 was in agreement with that of a natural thallium (Tl);

Table 5. Results of isotopic abundance analysis for SRM-981 (Number of samples n=13).

	Isotopic abundance (%)			
	Pb-204	Pb-206	Pb-207	Pb-208
Measured	1.4258±0.0025	24.1415±0.0243	22.0872±0.0042	52.3455±0.0277
Certificated	1.4255±0.0006	24.1442±0.0029	22.0833±0.0014	52.3470±0.0043

therefore, it was concluded that the prepared Pb sample contained Tl as an impurity. This is why we should consider isobaric interference due to ^{205}Tl in deriving the neutron capture cross-section of the ^{204}Pb (n,γ)^{205}Pb reaction with an isotopic ration of ^{205}Pb/^{204}Pb. There are only two isotopes in natural thallium: ^{203}Tl and ^{205}Tl, and their natural abundance are evaluated by the Commission of Isotopic Abundances and Atomic Weights, which is a suborganization within the International Union of Pure and Applied Chemistry (IUPAC) [22]. The isotopic ratio between ^{205}Tl and ^{203}Tl is given as:

$$\left(^{205}\mathrm{Tl}/_{^{203}\mathrm{Tl}}\right)_{nat.} = 2.387. \tag{3}$$

Let symbol $^{203}\mathrm{Tl}_{obs}$ be a yield of ^{203}Tl observed in a mass spectrum, $^{205}\mathrm{Tl}^{*}$ be the expected yield of ^{205}Tl, and ^{205}X be the yield observed at a mass number of 205. Assuming that Tl was contained in the Pb sample as an impurity with its natural abundances, it can be written as:

$$\left(^{205}\mathrm{Tl}^{*}/_{^{203}\mathrm{Tl}_{obs.}}\right) = \left(^{205}\mathrm{Tl}/_{^{203}\mathrm{Tl}}\right)_{nat.} \tag{4}$$

From Eq. (4), the yield of ^{205}Tl in the Pb sample can be estimated by:

$$^{205}\mathrm{Tl}^{*} = {}^{203}\mathrm{Tl}_{obs.} \cdot \left(^{205}\mathrm{Tl}/_{^{203}\mathrm{Tl}}\right)_{nat.} = 2.387 \cdot {}^{203}\mathrm{Tl}_{obs.} \tag{5}$$

The net yield of ^{205}Pb could be easily derived as follows:

$$^{205}\mathrm{Pb} = {}^{205}\mathrm{X} - {}^{205}\mathrm{Tl}^{*}. \tag{6}$$

Consequently, the net isotopic ratio ^{205}Pb/^{204}Pb can be obtained by:

$$^{205}\mathrm{Pb}/_{^{204}\mathrm{Pb}} = \left({}^{205}\mathrm{X} - {}^{205}\mathrm{Tl}^{*}\right)/{}^{204}\mathrm{Pb}. \tag{7}$$

The generation of ^{205}Pb by neutron irradiation of the ^{204}Pb sample is given by the following equation using ^{205}Pb/^{204}Pb ratios before and after the irradiations:

$$\left[\left({}^{205}\mathrm{X} - {}^{205}\mathrm{Tl}^{*}\right)/{}^{204}\mathrm{Pb}\right]_{after} - \left[\left({}^{205}\mathrm{X} - {}^{205}\mathrm{Tl}^{*}\right)/{}^{204}\mathrm{Pb}\right]_{before}. \tag{8}$$

Here, a difference is taken in order to prevent the ^{205}Tl from being missed and/or overtaken, because the term $[(^{205}\mathrm{X} - {}^{205}\mathrm{Tl}*)/{}^{204}\mathrm{Pb}]_{before}$ in Eq. (8) might not become zero ascribe to the analysis uncertainties. The obtained mass spectrum is drawn in Figure 5; the spectrum of the non-irradiated Pb sample is also plotted in Figure 5 so that the changes in the spectra can be clearly seen before and after the irradiation. Table 6 summarizes the results of isotopic ratios of the Pb samples before and after the irradiation, and the values in the sample spec sheet are also listed. The present analysis found the net isotopic ratio ^{205}Pb/^{204}Pb to be $(8.422 \pm 0.367) \times 10^{-5}$, and the ratio as small as 5 orders of magnitude could be measured with an uncertainty of about 4.3%. It would be a future task to improve the uncertainty by an order of magnitude by examining additives in mass spectrometry [21].

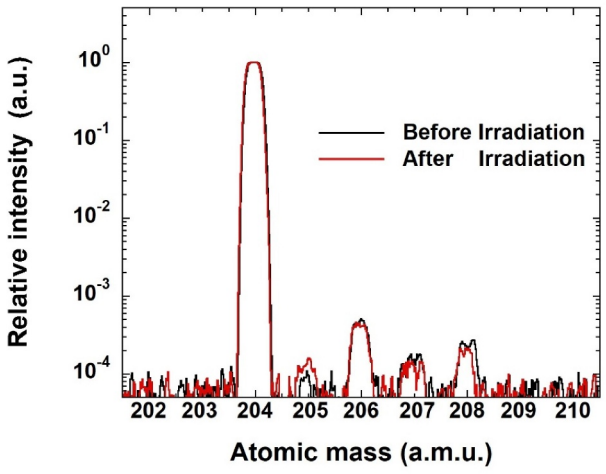

Figure 5. Mass spectrum for irradiated ^{204}Pb sample. Figure also draws the spectrum for the non-irradiated ^{204}Pb sample.

Table 6. Result of the isotopic abundance analysis of ^{204}Pb samples before and after the irradiation.

	Isotopic abundance (%)		
Lead isotope	Certificate sheet	Before irradiation	After irradiation
Pb-204	99.94	99.9392 ± 0.0039	99.9305 ± 0.0023
Pb-206	0.04	0.0375 ± 0.0010	0.0365 ± 0.0003
Pb-207	0.01	0.0084 ± 0.0011	0.0088 ± 0.0008
Pb-208	0.01	0.0148 ± 0.0021	0.0158 ± 0.0011
Pb-205			0.0084 ± 0.0004

4. Results and discussions

The number of ^{205}Pb produced by neutron irradiation of ^{204}Pb is given by the following equation:

$$n_1 = \frac{1}{\lambda} n_0 \sigma \phi (1 - \exp(-\lambda T_{irr})), \tag{9}$$

where n_0 and n_1 are the numbers of nuclei of ^{204}Pb and ^{205}Pb; σ is the neutron capture cross-section of^{204}Pb; Φ is the neutron flux; λ is the decay constant of ^{205}Pb; T_{irr} is the irradiation time (576 hours). It is naturally conceivable that the produced ^{205}Pb loses its production due to neutron absorption. Using the thermal-neutron capture cross-section of 4.50 barns adopted in JENDL-5.0, the loss to ^{205}Pb production was estimated to be at most 0.035%. This is why the double neutron capture reaction of ^{204}Pb was not considered here. Since the half-life of ^{205}Pb is as long as $(1.73 \pm 0.07) \times 10^7$ years [4], $(1.53 \pm 0.07) \times 10^7$ years [12] and $(1.70 \pm 0.09) \times 10^7$ years [23], the ^{205}Pb nucleus can be treated as a stable nuclide in the time span in this experiment. The difference between the half-lives used in the analysis affects the result of the reaction rate in the conventional activation method, but the half-life can be ignored under the present condition: $\lambda T_{\mathrm{irr}} \sim 3 \times 10^{-9} << 1$. Hence, Eq. (9) can be written more simply by:

$$n_1 = n_0 \sigma \phi T_{irr} = n_0 R T_{irr}, \tag{10}$$

where σΦ is replaced with the reaction rate R. The term of the number of nuclei in Eq. (10) is transformed and expressed in the form of the ratio between ^{205}Pb and ^{204}Pb as:

$$n_1/n_0 = R T_{irr}. \tag{11}$$

The reaction rate can be derived only from the isotopic ratio and irradiation time. The obtained isotopic ratio $(8.42 \pm 0.37) \times 10^{-5}$ was divided by the irradiation time (576 hours) to find the reaction rate R as $(4.06 \pm 0.18) \times 10^{-11}$1/sec. The self-shielding coefficient G_{th} was estimated to be unity. Assuming the g factor of unity, the division of the reaction rate R by the neutron flux discussed in *Subsection 3.1* gives the thermal-neutron capture cross section of ^{204}Pb as 0.536 ± 0.030 barns.

The present result is compared with the previous experimental values [24–26] and evaluated data [15,27–32] in Table 7. While the evaluated values of Refs [15,29,30,32] are close to the experimental values given by Jurney *et al.* [26], those of Refs [27,28,31] are close to the value given by Wing *et al.* [25] The latest evaluated nuclear data library JENDL-5 [32] shows the thermal-neutron capture cross-section of 703.1 mb for ^{204}Pb together with the energy-dependent neutron capture cross-section data based on the neutron capture cross-section data from 1 eV to 440 keV by Domingo-Pardo *et al.* [33]. In a previous measurement at the Oak Ridge National Laboratory [24], the neutron capture cross-sections were systematically measured for more than 100 isotopes. Using the pile oscillator method [34,35], the neutron capture cross-section of ^{204}Pb was derived as 0.9 ± 0.6 barns with an uncertainty of 70%. This value is largest among the cross sections measured so far. Wing *et al.* [25] derived the neutron capture cross-section of 0.7 ± 0.2 barns with a 28% uncertainty using the mass spectrometry, which was similar to the present measurement

Table 7. Present result of the thermal-neutron capture cross-section for ^{204}Pb together with the previously reported and evaluated data.

Author	Year	σ_0 (barn)	Method	Ref.
This work	—	0.536 ± 0.030	Activation & mass analysis	
JENDL-5	2021	0.7031	*Evaluation*	[32]
ENDF/B-VIII.0	2018	0.6609	*Evaluation*	[31]
Mughabghab	2018	0.703 ± 0.035	*Evaluation*	[15]
JEFF-3.3	2017	0.7036	*Evaluation*	[30]
JENDL-4.0	2011	0.7032	*Evaluation*	[29]
ENDF/B-VII.1	2011	0.6609	*Evaluation*	[28]
Mughabghab	1984	0.661 ± 0.07	*Evaluation*	[27]
Jurney *et al.*	1967	0.661 ± 0.070	Capture gamma-ray analysis	[26]
Wing *et al.*	1958	0.7 ± 0.2	Activation & Mass analysis	[25]
Pomerance	1952	0.9 ± 0.6	Pile oscillator method	[24]

method. Although they irradiated the Pb sample in the reactor for a long period, neutron fluxes were not measured. Instead, those were calculated by reducing the values from the pile data by 20%. In addition, they performed mass analysis after chemical treatment by adding Tl, Bi, Hg, Sn, Sb, and Fe as hold back carriers to the irradiated Pb sample. As described in the previous section, the ^{205}Tl impurity contributes to the yield of the mass number of 205 in the mass spectrum. This isobaric interference has been carefully considered when the neutron capture cross section of ^{204}Pb is derived by mass spectrometry. Jurney *et al.* [26] derived the neutron capture cross-section of ^{204}Pb by capture gamma-ray analysis. A ^{204}Pb sample enriched to 74.1% including ^{206}Pb (11.8%), ^{207}Pb (5.9%), and ^{208}Pb (8.2%) was irradiated with neutrons. By taking the sum of the partial cross sections over all the observed gamma rays, they extracted the neutron capture cross-section of 0.661 ± 0.070 barns [26] which is slightly larger than the present one.

In the future, we plan to apply the present measurement technique to other stable Pb isotopes such as ^{206}Pb and ^{207}Pb. Accurate thermal-neutron capture cross sections of these Pb isotopes can be used to normalize their energy-dependent cross-section data.

5. Conclusion

Lead is used as a coolant for the fast reactor proposed in the GEN-IV; Pb contains ^{204}Pb isotope. Another Pb isotopes only produce stable or short half-life nuclides through neutron capture reaction, but ^{204}Pb does a long-lived radioactive nuclide: ^{205}Pb. From the viewpoint of activation of ^{204}Pb, the cross-section measurement was conducted for ^{204}Pb. However, its cross-section measurement was difficult by the conventional activation method using neutrons supplied from a nuclear reactor due to the weak radioactivity of ^{205}Pb. Thereupon, we have come up with the idea that the neutron capture cross-section could be derived if the Pb isotopic ratios could be measured by mass spectrometry. The isotopic ratio was measured with high accuracy (10^{-5}) by devising additives and considering isotope interference. The present work succeeded in measuring the thermal-neutron capture cross-section of ^{204}Pb using the highly enriched ^{204}Pb sample by mass spectrometry, and found it to be 0.536 ± 0.030 barns. The present result revealed that the past experimental value [26] was overestimated by 18%; it was adopted as the evaluated data [27,31] though. Furthermore, the latest evaluated data [29,30,32] might be overestimated by 24%. It is expected that the present result would be adequately evaluated and the evaluated nuclear libraries would be revised.

Acknowledgments

The authors would like to greatly appreciate the staff working in the JRR-3 for their cooperation and acknowledge Mrs. Atsushi Yamaguchi, Toshiyuki Takahashi, Masayuki Fujita, and Yuji Sekiya of the facility management section, and Katsuhiko Ishizaki of the JRR3 management section. One of the authors (S.N.) would also like to express gratitude to Dr Osamu Iwamoto of JAEA for their constructive comments and for carefully proofreading the manuscript.

References

[1] Generation-IV International Forum (GIF) on the web (May12th, 2022). Available from: https://www.gen-4.org/gif/
[2] A Technology Roadmap for Generation IV Nuclear Energy Systems. U.S.A.: U.S.DOE Nuclear Energy Research Advisory Committee and the Generation IV International Forum; 2002, GIF-002-00.
[3] Salvatores M, Jacqmin, R. Uncertainity and target accuracy assessment for innovative systems using recent covariance data evaluations. Report NEA/WPEC-26, Paris (2008).
[4] Nuclide-LARA [Internet]. France: Laboratoire National Henri Becquerel; [cited 2022 April 26].
[5] The Japan Research Reactor-3 (JRR-3) [Internet]. Japan: Japan Atomic Energy Agency; [cited 2022 May 12]. Available from: https://jrr3.jaea.go.jp/jrr3e/index.htm
[6] Shibahara Y, Kubota T, Fujii T, et al. Analysis of cesium isotope compositions in environmental samples by thermal ionization mass spectrometry-1. A preliminary study for source analysis of radioactive contamination in Fukushima prefecture. J Nucl Sci Technol. 2014;51(5):575–579. DOI:10.1080/00223131.2014.891954
[7] Shibahara Y, Kubota T, Fujii T, et al. Analysis of cesium isotope compositions in environmental samples by thermal ionization mass spectrometry-3. Measurement of isotopic ratios of Cs in soil samples obtained in Fukushima prefecture. J Nucl Sci Technol. 2017;54(2):158–166. DOI:10.1080/00223131.2016.1223560
[8] Shibahara Y, Nakamura S, Uehara A, et al. Measurement of cesium isotopic ratio by thermal ionization mass spectrometry for neutron capture reaction studies on ^{135}Cs. J Radioanal Nucl Chem. 2020;325(1):155–165. DOI:10.1007/s10967-020-07198-2
[9] Institute for Integrated Radiation and Nuclear Science, Kyoto University [Internet]. Osaka: Kyoto University; [cited 2022 May 12]. Available from: https://www.rri.kyoto-u.ac.jp/en/facilities/kur
[10] Croff AG. ORIGEN2: A Versatile Computer Code for Calculating the Nuclide Compositions and Characteristics of Nuclear Materials. Nucl Technol. 1983;62(3):335–352.
[11] Nakamura S, Shibahara Y, Endo S et al. Thermal-Neutron Capture Cross Sections and Resonance Integrals of the ^{243}Am(n,γ)^{244g}Am and ^{243}Am(n,γ)$^{244m+g}$Am Reactions. J Nucl Sci Technol. 2021;58(3):259–277.
[12] Firestone RB, Shirley VS, Baglin CM, et al. Table of Isotopes 8th. updated. New York: John Wiley and Sons; 1998.

[13] Westcott CH, Walker WH, Alexander TK Proceedings of Second International Conference *Peaceful Uses Atomic Energy*, Geneva, 1958; 16: p.70.
[14] Walker WH, Westcott CH, Alexander TK. MEASUREMENT of RADIATIVE CAPTURE RESONANCE INTEGRALS in a THERMAL REACTOR SPECTRUM, and the THERMAL CROSS SECTION of Pu-240. Can J Phys. 1960;38(1):57.
[15] Mughabghab SF. Atlas of Neutron Resonances 6*th ed*. Vol. 1 and 2. Netherlands: Elsevier Science; 2018.
[16] Nakamura S, Shibahara Y, Kimura A, et al. Measurements of thermal-neutron capture cross-section of cesium-135 by applying mass spectrometry. J Nucl Sci Technol. 2020;57 (4):388–400. DOI:10.1080/00223131.2019.1691077
[17] Platzner IT. Modern isotope ratio mass spectrometry. Chichester: Willey; 1997.
[18] Catanzaro EJ, Murphy TI, Shields WR, et al. Absolute isotopic abundance ratios of common, equal-atom, and radiogenic lead isotopic standards. J. Res. Nat. Bur. Std. 1968;72A(3):261–267. DOI:10.6028/jres.072A.025
[19] Todt W, Cliff RA, Hanser A et al. Evaluation of a ^{202}Pb-^{205}Pb double spike for high precision lead isotope analysis, Earth Processes: reading the Isotopic Code. Geophysical Monograph. 1996;95:429-437. DOI:10.1029/GM095p0429
[20] Gerstenberger H, Haase G. A highly effective emitter substance for mass spectrometric Pb isotope ratio determinations. Chem Geol. 1997;136(3–4):309–312.
[21] Huyskens MH, Iizuka T, Amelin Y et al. Evaluation of colloidal silica gels for lead isotopic measurements using thermal ionization mass spectrometry. J Anal At Spectrom. 2012;27(9):1439–1446.
[22] Meija J, Coplen TB, Berglund M et al. Isotopic compositions of the elements 2013. Pure Appl Chem. 2016; 88(3): 293–306International Union of Pure and Applied Chemistry (IUPAC)Internet[cited 2022 May 12]. Available from. doi:10.1515/pac-2015-0503
[23] Kondev FG. Nuclear Data Sheets for A=205. Nucl Data Sheets. 2020;166:1–230.
[24] Pomernce H. Thermal neutron capture cross section. Phys Rev. 1952;88(2):412–413.
[25] Wing J, Stevens CM, Huizenga JR. Radioactivity of lead-205. Phys Rev. 1958;111(2):590–592.
[26] Jurney ET, Motz HT. Gamma-ray spectrum from ^{204}Pb(n,γ)^{205}Pb. Nucl Phys A. 1967;94:351–365.
[27] Mughabghab SF. Neutron Cross Sections. Vol. 1. New York: Academic Press; 1984. Part B
[28] Chadwick MB, Herman M, Obložinský P, et al. ENDF/B-VII.1 nuclear data for science and technology. cross sections, covariances, fission product yields and decay data. Nucl Data Sheets. 2011;112 (12):2887–2996. DOI:10.1016/j.nds.2011.11.002
[29] Shibata K, Iwamoto O, Nakagawa T, et al. J. JENDL-4.0: a New Library for Nuclear Science and Engineering. J Nucl Sci Technol. 2011;48(1):1–30. DOI:10.1080/18811248.2011.9711675
[30] Plompen AJM, Cabellons O, De SJC, et al. The joint evaluated fission and fusion nuclear data library, JEFF-3.3. Eur Phys J A. 2020;56(7):181. DOI:10.1140/epja/s10050-020-00141-9
[31] Brown DA, Chadwick MB, Capote R, et al. ENDF/B-VIII.0: the 8*th* Major Release of the Nuclear Reaction Data Library with CIELO-project Cross Sections, New Standards and Thermal Scattering Data. Nucl Data Sheets. 2018;148:1–142.
[32] Iwamoto O. Japanese Evaluated Nuclear Data Library version 5: jENDL-5. [to *be published in J. Nucl. Sci. Technol.*]
[33] Domingo-Pardo C, Abbondanno U, Aerts G, et al. Measurement of the neutron capture cross section of the s-only isotope $Pb^{204}$from 1 eV to 440 keV. Phys Rev C. 2007;75(1):015806. DOI:10.1103/PhysRevC.75.015806
[34] Hoover JI, Jordan WH, Moak CD, et al. Measurement of neutron absorption cross sections with a pile oscillator. Phys Rev. 1948;74(8):864–870. DOI:10.1103/PhysRev.74.864
[35] Pomerance H. Thermal neutron capture cross sections. Phys Rev. 1951;83(3):641–645.